



HAL
open science

Thermal performance of carbon nanotube nanofluids in solar microchannel collectors: an experimental study

Selim Ahlatli, Thierry Maré, Patrice Estellé, Nimeti Doner

► To cite this version:

Selim Ahlatli, Thierry Maré, Patrice Estellé, Nimeti Doner. Thermal performance of carbon nanotube nanofluids in solar microchannel collectors: an experimental study. *International Journal of Technology (IJTech)*, 2016, 2, pp.78-85. hal-01267168

HAL Id: hal-01267168

<https://hal.science/hal-01267168>

Submitted on 29 Feb 2016

HAL is a multi-disciplinary open access archive for the deposit and dissemination of scientific research documents, whether they are published or not. The documents may come from teaching and research institutions in France or abroad, or from public or private research centers.

L'archive ouverte pluridisciplinaire **HAL**, est destinée au dépôt et à la diffusion de documents scientifiques de niveau recherche, publiés ou non, émanant des établissements d'enseignement et de recherche français ou étrangers, des laboratoires publics ou privés.

THERMAL PERFORMANCE OF CARBON NANOTUBE NANOFLUIDS IN SOLAR MICROCHANNEL COLLECTORS: AN EXPERIMENTAL STUDY

Selim Ahlatli¹, Thierry Mare^{2*}, Patrice Estelle³, Nimet Doner¹

¹ Department of Mechanical Engineering, Dumlupinar University, 43270 Kutahya, Turkey

² LGCGM EA3913, Equipe Matériaux et Thermo-Rhéologie, Université Rennes 1, IUT de Saint-Malo, Rue de la Croix Désilles, CS51713, 35417 Saint - Malo Cedex, France

³ LGCGM EA3913, Equipe Matériaux et Thermo-Rhéologie, Université Rennes 1, IUT de Rennes, 3 rue du Clos Courtel, BP 90422, 35704 Rennes Cedex 7, France

(Received: August 2015 / Revised: January 2016 / Accepted: January 2016)

ABSTRACT

Many studies show that nanofluids, especially with carbon nanotubes, improve heat transfer. Other studies show that a nanofluid is a good candidate for solar systems because of its good absorptivity. We are facing an increasing number of miniaturized and more powerful systems. Especially in microelectronics, small heat sinks with high heat transfer are being developed, called micro-channel heat sinks (MCHS). In this paper, the heat transfer behavior of carbon nanotube–water nanofluid in a microchannel solar collector is studied experimentally. The exchanger is composed of 16 micro-channel hydraulic diameters of 1 mm and a glass or quartz cover with a surface area of 25 cm². Solar radiation is simulated by a halogen lamp. The experimental set-up includes a solar meter, pressure, and temperature sensors, and it is allowed to control the flow. The nanofluid is a solution of water containing a 0.01%, 0.05%, 0.1%, and 0.5% weight fraction, respectively, of the carbon nanotubes, which are 9.2 nm in diameter and 1.5 μm in length. Viscosity and density are measured experimentally. The evolution of efficiency and the pressure drop are presented according to the Reynolds number and are compared with the results obtained with distilled water.

Keywords: Experimental; Nanofluid; CNT; Micro-Channel Heat Sink (MCHS); Solar collector; Pressure drop; Efficiency

1. INTRODUCTION

Nanofluids have been studied heavily and are good candidates for the improvement of heat transfer. Composed of solid nanoparticles in an aqueous medium, they greatly increase the thermal conductivity of the fluid obtained. Generally, nanoparticles can be classified according to their shapes: (i) spherical nanoparticles (copper, Cu; iron, Fe; gold, Au, silver, Ag; aluminum oxide, Al₂O₃; copper oxide, CuO; titanium oxide, TiO₂; etc.) and (ii) nanotubes (carbon nanotubes, CNT). The base fluids are usually water, oil, or water-ethylene glycol. Wang & Mujumdar (2007) compiled experimental results regarding the thermal conductivity of CNT-based nanofluids. Their results show an improvement of nanofluids' thermal conductivity compared to that of the base fluid depending on the volume fraction concentration. Similar experimental results regarding nanofluids' optic and fundamental properties have been published by Eastman et al. (2001), Garg et al. (2008), Zhang et al. (2014), and Otanicar et al. (2010). Carbon nanotubes are characterized by a large aspect ratio and high thermal

* Corresponding author's email: thierry.mare@univ-rennes1.fr, Tel.+33-2 99219505, Fax. +33- 299219541
Permalink/DOI: <http://dx.doi.org/10.14716/ijtech.v7i2.1575>

Conductivity (Karami et al., 2014; Koblinski et al., 2002). In addition, Mizuno et al. (2009) found that a CNT acts as a blackbody in the heat transfer mechanism.

The suspension of CNT implementation is usually accompanied by ultrasound, chemical, and mechanical processes with the use of a surfactant to homogenize the distribution of the CNT in the base fluid and to strengthen the stability of the suspension (Kohei et al., 2009; Yu & Huaqing, 2012). Phuoc et al. (2011) show experimentally that the dynamic viscosity of CNT nanofluids increases with the volume concentration. Many studies have shown that the dynamic viscosity of nanofluids decreases as the temperature increases (Aladag et al., 2012). Other effects may also influence the dynamic viscosity and rheological behavior of CNT-based nanofluids, such as the presence of agglomerates (Chen et al., 2013), thixotropic behavior (Estellé et al., 2013), and the synthesis methods of the CNT. Most recently, nanofluids with carbon-nanoparticles have also been suggested as working fluid because of their unique thermal and optical properties (Sabourin et al., 2009; Gan & Li, 2012). The other study has confirmed that the addition of the CNT can bring thermal gains with a relatively large performance (Maré et al., 2011).

We are facing an increasing number of miniaturized and more powerful systems. Especially in microelectronics, they develop small-size heat sinks with high heat transfer, called micro-channel heat (MCH). MCHS usually contains a large number of parallel micro-channels with hydraulic diameters ranging from 10 to 1000 μm . Gunnasegaran et al. (2010) numerically compared the effects of different cross-sections on heat transfer. They showed, with water as a transfer medium, that a rectangular cross-section is better than triangular or trapezoidal cross-sections. They also showed that the thermal resistance varies from 10% to 35% depending on the hydraulic diameter. Halelfadl et al. (2014) have recently shown from numerical optimization analysis that CNTs' water-based nanofluid as a working fluid reduces the total thermal resistance of MCHS and can significantly enhance the thermal performance of the working fluid, particularly at high temperatures. The performance of solar radiation absorption in a short wave by a CNT is demonstrated by Shende and Sundara (2015). Saeedinia et al., (2012) present a review of solar applications with a nanofluid. They confirm that the gain is 13% greater than that of a conventional fluid in solar applications. The experimental and numerical results demonstrate an initial rapid increase in efficiency with volume fraction, followed by a leveling off in efficiency as the volume fraction continues to increase (Himanshu et al., 2009). Faizal et al. (2013a) and Faizal et al. (2013b) evaluated the potential of four different water-based nanofluids, including nanoparticles such as CuO , SiO_2 , TiO_2 , and Al_2O_3 , to reduce the size of solar collectors. They concluded that CuO and Al_2O_3 /water nanofluids are the best option for reducing the size of solar collectors.

The flow and heat transfer research of the MCHS can help with estimating the thermal performance and optimizing the design of MCHS. The aim of the present study is to investigate the use of nanofluid-CNT with a low weight fraction as a working fluid in a solar collector. The exchanger is composed of 16 micro-channel hydraulic diameters of 1 mm, and its total surface area is 25 cm^2 . Solar radiation is simulated by a halogen lamp of 100 W. The experimental setup consists of a solar meter, pressure, and temperature sensors, and it is allowed to control the flow. The nanofluids are a solution of water containing a 0.01%, 0.05%, 0.1%, and 0.5% weight fraction, respectively, of CNTs that are 9.2 nm in diameter and 1.5 μm in length. Viscosity and density are measured experimentally. In this study, the results of the nanofluids of two weight fractions are presented. The evolutions of heat flux and pressure drop are presented according to the Reynolds number and are compared with the results obtained with distilled water.

2. DISPARITY LINE UTILIZATION FACTOR

The nanofluid presently investigated consists of multi-walled CNTs (purity of 90%) of 1.5 μm in average length and 9.2 nm in average diameter dispersed in a mixture of deionized water and sodium polycarboxylate as a surfactant. The nanotube weight fraction varies from 0–0.5%. Due to the true density of nanotubes, this corresponds to a volume fraction of 0–0.278%.

The nanofluid was obtained from the dilution of a starting suspension containing 1% in the weight fraction of the nanotubes and 2% in the weight fraction of the surfactant initially prepared by Nanocyl. Mechanical stirring was also applied to the diluted nanofluid to ensure the nanotubes' dispersion. Measurements of density in the continuation of this work are made using a tube densimeter vibrating Anton PAAR coupled with a cell DMA 602, which allows for accuracy of the order of 1.10^{-5} g/cm^3 .

The specific heat is based on the assumption of thermal equilibrium between the particles and the base fluid (O'Hanley et al., 2012) confirmed experimentally with a calorimeter differential scanning rather than with the valid Equation 1 for concentrations less than 1%. The specific heat is defined as following in Equation 1.

$$C_{p,nf} = \frac{\varphi_v (\rho C_p)_{np} + (1 - \varphi_v) (\rho C_p)_{bf}}{\varphi_v \rho_{np} + (1 - \varphi_v) \rho_{bf}} \quad (1)$$

Rheological measurements of the nanofluid are conducted with a Kinexus Pro-rheometer (Malvern) with a well-controlled temperature under $\pm 0.01^\circ\text{C}$. The comprehensive experimental procedure is detailed in Estellé et al., (2014). The maximum deviation in viscosity measurement was previously evaluated to 3%. Experimental data of the nanofluids are presented in Table 1.

Table 1 Physical properties of the nanofluid

Weight fraction (%)	Density (kg/m^3)	Viscosity (Pa.s)	Specific heat (kJ/kg.K)
0	1000	0.001	4.18179
0.01	1000.52	0.001	4.18179
0.05	1000.69	0.001016	4.180065
0.1	1001.45	0.001	4.17809
0.5	1004.643	0.00225	4.17218

3. MICRO-CHANNEL HEAT SINK

3.1. Objective Function

The experimental set-up is presented in Figure 1. In the setup, the components are connected by tubes to a thermal-controlled bath[Ⓜ] and centrifugal pump[Ⓜ] to regulate the flow rate. Platinum probes with a maximum accuracy of 0.1°C are inserted into the flow at the inlet (T_i) and outlet (T_o) of each tube[Ⓜ]. In addition, two pressure sensors with an accuracy of 1% are also connected to the inlet (P_i) and the outlet (P_o)[Ⓜ]. The flow rate ranging from 0–150 ml/min is measured directly from the time required to accumulate a fixed volume of the nanofluid using a three-way valve[Ⓜ], with an accuracy of 1 ml/min. All of the data are connected to a data acquisition system (Labview). To minimize heat loss, all pipes and MCHS are covered with a 4 cm-thick insulating material (thermal conductivity of 0.04 W/mK). The micro-channel heat sink is depicted in Figure 2. It is made of copper and has sixteen $1\text{mm} \times 1\text{mm}$ parallel square cross-section channels. The total dimensions are $150\text{mm} \times 70\text{mm} \times 15\text{mm}$. Two transparent surfaces[Ⓜ]

of thickness 4 mm, glass and quartz, are placed on a surface of 0.00785 m^2 with a gap of 2 mm. The lamp[®] placed at 30 cm is a Philips Halogen A PAR38 100 W lamp, used to simulate the solar spectrum in the experimental setup. Radiation is measured by the solar meter "KippzonSp lite 2," with a precision of 0.15%.

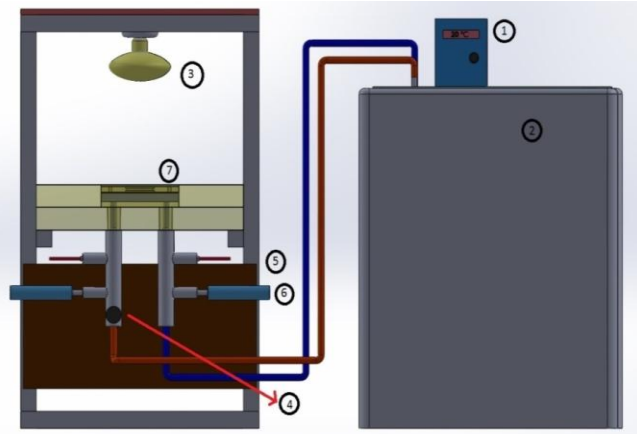


Figure 1 Experimental setup

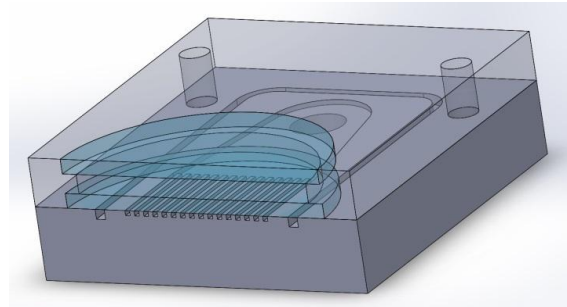


Figure 2 Schematic picture of MCHS

3.2. Reduction of Loss

The Reynolds number is given by the following Equation 2:

$$\text{Re} = \frac{\rho_f V_f D_H}{\mu_f} \quad (2)$$

where V_f and D_H are the fluid velocity within a channel and the hydraulic diameter of the same channel, respectively. The heat transfer rate in the MCHS is defined in Equation 3 as:

$$\Phi = \rho_f q C_p (T_i - T_o) \quad (3)$$

The pumping power is defined by Equation 4 using the pressure drop (ΔP) and flow rate (q).

$$P(w) = \Delta p \cdot q \quad (4)$$

4. RESULTS AND DISCUSSION

Nanofluids having weight fractions of 0.05 and 0.5% carbon nanotubes were used for comparison. Water was selected as the base fluid. We investigated the effects of pumping power, heat transfer, and pressure drop on the heat and flow characteristics of nanofluids by experimental study. In addition, glass and quartz were tested to show how the absorption of sunlight is affected. The measured pumping power of the base water and two concentrations of nanofluids with glass and quartz are shown in Figures 3a and 3b. The results show that the pumping power increases when the Reynolds number increases in all of the studied cases. The pumping power of the nanofluid at a 0.5% weight fraction is higher than those of the nanofluid with the lower weight fraction and the base fluid under the same conditions. These results are consistent with experimental results of the heat transfer characteristics of CuO-based oil nanofluids (Sabourin et al., 2009).

As can be seen from Figures 3a and 3b, the pumping power of MCHS is strongly affected by the weight fraction of the nanofluid and the type of glass at the top of the heat exchanger. Almost identical results were obtained for the nanofluid at a weight fraction of 0.05% and the base fluid; however, the pumping power of the nanofluid at a 0.5% weight fraction is found to

be much bigger than in the other two cases. The variations of the heat transfer as a function of the Reynolds number for the studied fluids when using glass and quartz are given in Figures 4a and 4b, respectively. The radiation is transmitted through the glass or quartz at the top surface of the heat exchanger. When the nanofluid is exposed to the radiation generated from the halogen lamp, most of the radiation energy is reflected into the MCHS surface. Radiation absorption by both the base fluid and the suspended CNT can enhance the heat transfer.

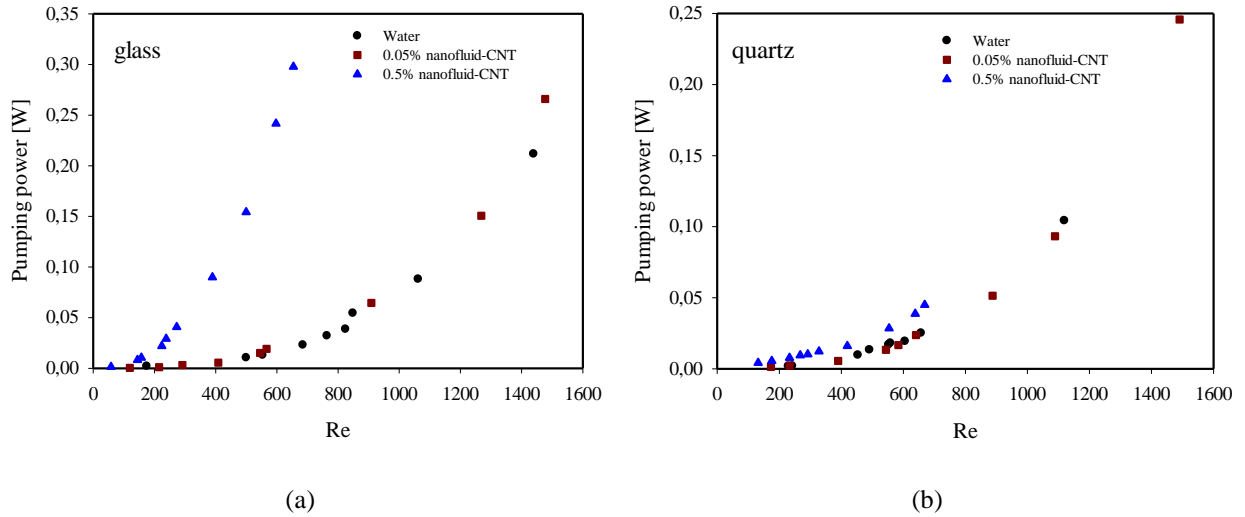


Figure 3 Comparison of pumping power for MCHS for water and the studied nanofluids: (a) glass; and (b) quartz

From Figures 4a and 4b, it is obvious that the heat transfer of the nanofluids is much bigger than that of the base fluid for both types of glass (quartz and glass), as mentioned in Gan & Li (2012).

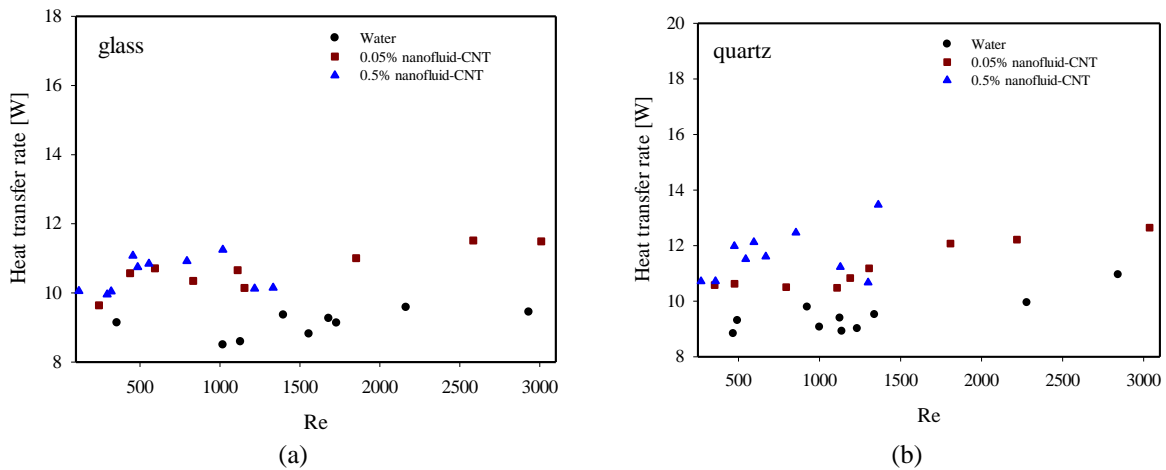


Figure 4 Comparison of heat transfer rate for MCHS: (a) glass; and (b) quartz

In addition, it can be seen that the heat transfer is augmented as the weight fraction of the nanofluid increases. It is shown that aggregation rarely occurred in the nanofluid with a low weight fraction because of the flow regime and viscosity of the nanofluid. In our study, results for the base fluid were compared with those of the studied nanofluids for the measured heat transfer and pressure drop. When the top surface of the MCHS was covered with quartz glass, an enhancement of the heat transfer was obtained: An average increase in heat transfer of

19.5% for the 0.05% weight fraction and an average increase of 25% for the 0.5% weight fraction were found. It can be concluded that the efficiency of heat transfer was improved by between 5 and 7% by using quartz as compared to glass. This enhancement of the heat transfer was caused by the radiative properties of quartz glass during the absorption and transmission process, as analyzed by Trukhin (2009). Moreover, it is seen that the heat transfer is increased with the increase of the Reynolds number. These results indicate that more radiation energy may be absorbed and will dissipate in the nanofluids with CNTs when compared with the base water, as mentioned in Mizuno et al. (2009).

The variation of the measured pressure drop as a function of the Reynolds number for the base fluid and nanofluids with two weight fractions with glass and quartz are given in Figures 5a and 5b, respectively. As can be seen from Figures 5a and 5b, the nanofluid with a 0.5% weight fraction has the highest pressure drop values compared to the base fluid and the nanofluid with a 0.05% weight fraction for both types of glass.

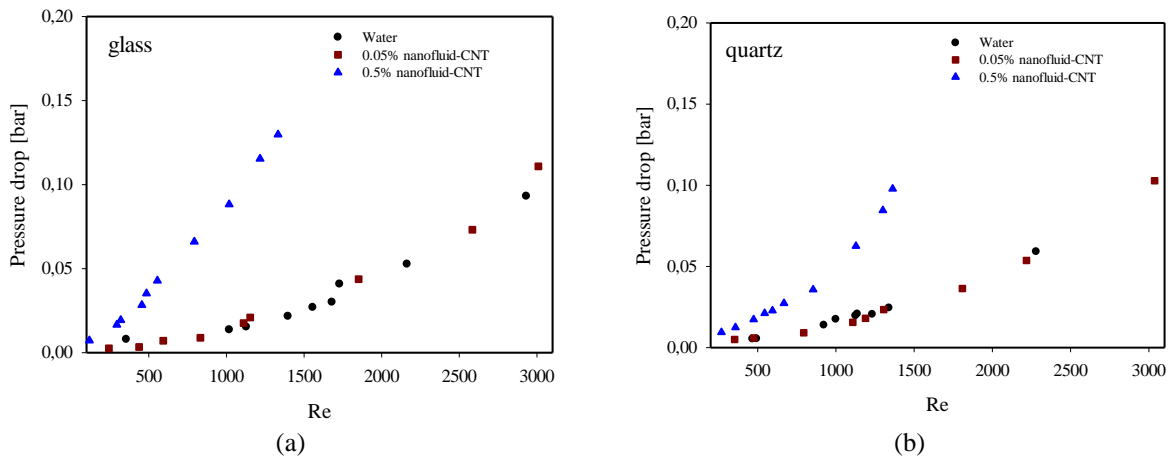


Figure 5 Comparison of pressure drop for MCHS: (a) glass; and (b) quartz

Also, the pressure drop of the nanofluids increases when the Reynolds number increases, as reported by Aladag et al. (2012) and Halefadi et al. (2015). With regard to the pressure drop, almost identical results were obtained for the nanofluid at a 0.05% weight fraction and the base fluid, with similar pumping power and heat transfer. When quartz is used at the top surface of the MCHS, the nanofluid with a high weight fraction has a lower pressure drop than when glass is used. The trend of a pressure drop is linear for glass, while it becomes exponential for quartz with the same nanofluid. In total, 250 experimental performances were studied. The aggregation of nanofluid at a 0.5% weight fraction was observed in these studies. However, the reason for this problem in the MCHS was not determined, but the following could be possible reasons: the limited number of experimental studies, the weight fraction of the nanofluid, the sensitivity of devices, and the flow regime in the channels. The next studies on this problem could focus on a detailed analysis of each of the above effects individually.

5. CONCLUSION

In this study, to evaluate the heat transfer and flow characteristics of nanofluids in MCHS, CNT nanofluids of 0.05 and 0.5% were used. As the weight fraction of nanofluids increased, the measured heat transfer, pump power, and pressure drop increased. The heat transfer of nanofluids is higher than that of the base fluid. The high-weight-fraction nanofluids become more effective when quartz is used at the top surface of the heat exchanger. We have concluded

that the heat transfer and the flow characteristics of the studied nanofluids are in accord with the findings of earlier studies in the literature.

6. NOMENCLATURE

Greek letters:

Φ	Concentration, %
ρ	Density, kg/m ³
μ	Viscosity, Pa.s
ϕ	Heat transfer flux, W

Indices:

nf	Nanofluid
V	Volume
np	Nanoparticle
f	Fluid
i	Inlet
o	Outlet

Symbols:

Re	Reynolds number
T	Temperature, °C
P	Pressure, Pa
v	Velocity, m/s
q	Flow rate, m ³ /s
Cp	Heat capacity, J/kgK

7. REFERENCES

- Aladag, B., Halelfadl, S., Doner, N., Maré, T., Duret, S., Estellé, P., 2012. Experimental Investigations of the Viscosity of Nanofluids at Low Temperatures. *App. Energy*, Volume 97, pp. 876–880
- Chen, F.L., Yang J.C., Zhou, W., He, Y., Huang, Y., Jiang, B., 2013. Experimental Study on the Characteristics of Thermal Conductivity and Shear Viscosity of Viscoelastic-fluidbased Nanofluids Containing Multiwalled Carbon Nanotubes. *Thermochimica Acta*, Volume 556, pp. 47–53
- Eastman, J.A., Choi, S.U.S., Li, S., Yu, W., Thompson, L.J., 2001. Anomalously Increased Effective Thermal Conductivities of Ethylene Glycol-based Nanofluids Containing Copper Nanoparticles. *Applied Physics Letters*, Volume 78(6), pp. 718–720
- Estellé, P., Halelfadl, S., Doner, N., Maré, T. 2013. Shear History Effect on the Viscosity of Carbon Nanotubes Water-based Nanofluid. *Current Nanoscience*, Volume 9(2), pp. 225–230
- Estellé, P., Halelfadl, S., Maré, T., 2014. Lignin as Dispersant for Water-based Carbon nanotubes Nanofluids: Impact on Viscosity and Thermal Conductivity. *International Communications in Heat and Mass Transfer*, Volume 57, pp. 8–12
- Faizal, M., Saidur, R., Mekhilef, S., 2013b. Potential of Size Reduction of Flat-plate Solar Collectors when Applying MWCNT Nanofluid. In: *the Proceedings of the 4th International Conference on Energy and Environment (ICEE2013)*, IOP Publishing, Day Month, Location. doi:10.1088/1755-1315/16/1/012004
- Faizal, M., Saidurb, R., Mekhilef, S., Alim, M.A., 2013a. Energy, Economic and Environmental Analysis of Metal Oxides Nanofluid for Flat-plate Solar Collector. *Energy Conversion and Management*, Volume 76, pp.162–168
- Gan, Y., Li, Q., 2012. Optical Properties and Radiation-enhanced Evaporation of Nanofluid Fuels Containing Carbon-based Nanostructures. *Energy & Fuels*, Volume 26, pp. 4224–4230
- Garg, J., Poudel, B., Chiesa, M., Gordon, J.B., Ma, J.J., Wang, J.B., Chen, G., 2008. Enhanced Thermal Conductivity and Viscosity of Copper Nanoparticles in Ethylene Glycol Nanofluid. *Journal of Applied Physics*, Volume 103(7), 074301, pp1–6
- Gunnasegaran, P., Mohammed, H.A., Shuaib, N.H., Saidur, R., 2010. The Effect of Geometrical Parameters on Heat Transfer Characteristics of Microchannels Heat Sink with

- Different Shapes. *International Communications in Heat and Mass Transfer*, Volume 37, pp. 1078–1086
- Halelfadl, S., Adham, A.M., Mohd-Ghazali, N., Maré, T., Estellé, P., Ahmad, R., 2014. Optimization of Thermal Performance and Pressure Drop of a Rectangular Microchannel Heat Sink using Aqueous Carbon Nanotubes Based Nanofluid. *Applied Thermal Engineering*, Volume 62, pp. 492–499
- Himanshu, T., Phelan, P., Prasher, R., 2009. Predicted Efficiency of a Low-temperature Nanofluid-based Direct Absorption Solar Collector. *Journal of Solar Energy Engineering*, Volume 131(4), pp.1-7
- Karami, M., Bahabadi, M.A., Delfani, S., Ghozatloo, A., 2014. A New Application of Carbon Nanotubes Nanofluid as Working Fluid of Low-temperature Direct Absorption Solar Collector. *Solar Energy Materials and Solar Cells*, Volume 121, pp. 114–118
- Keblinski, P., Phillpot, S.R., Choi, S.U.S., Eastman, J.A., 2002. Mechanisms of Heat Flow in Suspensions of Nano-sized Particles (Nanofluids). *International Journal of Heat and Mass Transfer*, Volume 45(4), pp. 855–863
- Maré, T., Halelfadl, S., Sow, O., Estellé, P., Duret, S., Bazantay, F., 2011. Comparison of the Thermal Performances of Two Nanofluids at Low Temperature in a Plate Heat Exchanger. *Experimental Thermal and Fluid Science*, Volume 35(8), pp. 1535–1543
- Mizuno, K., Ishii, J., Kishida, H., Hayamizu, Y., Yasuda, S., Futaba, D.N., Hata, K., 2009. A Black Body Absorber from Vertically Aligned Single-walled Carbon Nanotubes. In: *the Proceedings of the National Academy of Sciences*, Volume 106(15), pp. 6044–6047
- O’Hanley, H., Buangiorno, J., McKrell, T., Hu, L.W., 2012. Measurement and Model Validation of Nanofluid Specific Heat Capacity with Differential Scanning Calorimetry. *Advances in Mechanical Engineering*, Volume 2012, pp. 1–6
- Otanicar, T.P., Phelan, P.E., Prasher, R.S., Rosengarten, G., Taylor, R.A., 2010. Nanofluid-Based Direct Absorption Solar Collector. *Journal of Renewable and Sustainable Energy*, Volume 2(3), pp 1–13
- Phuoc, T.X., Massoudi, M., Chen, R.H., 2011. Viscosity and Thermal Conductivity of Nanofluids Containing Carbon Nanotubes Stabilized by Chitosan. *International Journal of Thermal Sciences*, Volume 50, pp. 12–18
- Sabourin, J.L., Dabbs, D.M., Yetter, R.A., Dryer, F.L., Aksay, I.A. 2009. Functionalized Graphene Sheet Colloids for Enhanced Fuel/propellant Combustion. *ACS Nano*, Volume 3(12), pp. 3945–3954
- Saeedinia, M., Akhavan-Behabadi, M.A., Razi, P., 2012. Thermal and Rheological Characteristics of CuO–base Oil Nanofluid Flow Inside a Circular Tube. *International Communications in Heat and Mass Transfer*, Volume 39, pp. 152–159
- Shende, R., Sundara, R., 2015. Nitrogen Doped Hybrid Carbon Based Composite Dispersed Nanofluids as Working Fluid for Low-temperature Direct Absorption Solar Collectors. *Solar Energy Materials and Solar Cells*, Volume 140, pp. 9–16
- Trukhin, A.N., 2009. Luminescence of Polymorph Crystalline and Glassy SiO₂, GeO₂: A Short Review. *Journal of Non-Crystalline Solids*, Volume 355, pp. 1013–1019
- Wang, X.Q., Mujumdar, A.S., 2007. Heat Transfer Characteristics of Nanofluids: A Review. *International Journal of Thermal Sciences*, Volume 46, pp. 1-19
- Yu, W., Huaqing, X., 2012. A Review on Nanofluids: Preparation, Stability Mechanisms, and Applications. *Journal of Nanomaterials*, Volume 2012, pp. 1-17
- Zhang, H., Chen, H.J., Du, X., Wen, D., 2014. Photothermal Conversion Characteristics of Gold Nanoparticle Dispersions. *Solar Energy*, Volume 100, pp. 141–147